Astronomy & Astrophysics manuscript no. sminpap-astroph
January 6, 2016

Dust production in debris discs: constraints on the smallest grains

P. Thebault[1]

LESIA-Observatoire de Paris, UPMC Univ. Paris 06, Univ. Paris-Diderot, France

Received ; accepted

ABSTRACT

Context. The surface energy constraint puts a limit on the smallest fragment s_{surf} that can be produced after a collision. Based on analytical considerations, this mechanism has been recently identified as been potentially able to prevent the production of small dust grains in debris discs and cut off their size distribution at sizes larger than the blow-out size.
Aims. We numerically investigate the importance of this effect to find under which conditions it can leave a signature in the small-size end of a disc's particle size distribution (PSD). An important part of this work is to map out, in a disc at steady-state, what is the most likely collisional origin for μm-sized dust grains, in terms of the sizes of their collisional progenitors.
Methods. We implement, for the first time, the surface energy constraint into a collisional evolution code. We consider a typical debris disc extending from 50 to 100AU and two different stellar types. We also consider two levels of stirring in the disc: dynamically "hot" ($<e>$=0.075) and "cold" ($<e>$=0.01). For all cases, we derive s_{surf} maps as a function of target and projectile sizes, s_t and s_p, and compare them to equivalent maps for the dust-production rate. We then compute disc-integrated profiles of the PSD and estimate the imprint of the surface energy constraint.
Results. We find that the (s_p,s_t) regions of high s_{surf} values do not coincide with those of high dust production rate. As a consequence, the surface energy constraint has generally a weak effect on the system's PSD. The maximum s_{surf}-induced depletion of μm-sized grains is $\sim$ 30% and is obtained for a sun-like star and a dynamically "hot" case. For the e=0.01 cases, the surface energy effect is negligible compared to the massive small grain depletion induced by another mechanism: the "natural" imbalance between dust production and destruction rates in low-stirring discs identified by Thebault & Wu (2008).

Key words. planetary system – debris discs – circumstellar matter

1. Introduction

Circumstellar debris discs have been detected around main sequence stars because of the excess luminosity produced by μm- to mm-sized dust. Because of its relatively short lifetime, this dust cannot be primordial and is thought to be steadily replenished by a chain of erosive collisions starting from a reservoir of large, planetesimal-like, parent bodies (e.g. Wyatt, 2008; Krivov, 2010). In an idealized case, the size distribution of bodies within such a collisional cascade should settle toward a power law of the form $dN \propto s^q ds$, where the index q is close to -3.5 (Dohnanyi, 1969). Such a power law has the interesting characteristics that, while most of the disc's mass is contained in the biggest objects of the cascade, most of the geometrical cross section should be contained in the smallest grains of size s_{min}. This means that, at all wavelengths $\lambda \lesssim 2\pi s_{min}$, the disc's luminosity should be dominated by these smallest grains.

Determining s_{min} is thus of crucial importance. Luckily enough, for most stars, stellar radiation pressure imposes a "natural" minimum cut-off size that is, in principle, easy to estimate. Indeed, because this pressure is both $\propto 1/s$ and, like stellar gravity, $\propto 1/r^2$ (r being the radial distance to the star), there is a minimum size s_{blow} below which radiation pressure overcomes gravity and grains are quickly blown out from the system. Taking into account the fact that small grains are probably produced from parents bodies on Keplerian orbits, the criteria for estimating s_{blow} is given by $\beta(s_{blow}) = F_{Rad.Press.}/F_{grav.} = 0.5$ (for parent bodies on circular orbits). For typical astro-silicates (Draine, 2003), values for β range from $\sim 0.5\mu$m for solar-type stars to 2-10μm for late type A stars (Krivov, 2007) [1]. As a consequence, in scattered light, disc luminosities should always be dominated by grains close to s_{blow}, and, for A stars, s_{blow} grains should also dominate the thermal flux up to mid-IR wavelengths.

However, observations have sometimes challenged this simple view. Some discs have, for example, been found to contain important fractions of sub-micron grains below s_{blow} (Ardila et al., 2004; Fitzgerald et al., 2007; Johnson et al., 2012). While there does not seem to be one single straightforward scenario for the presence of such tiny particles, some possible explanations have been suggested. One of them is that, at very small sizes, the $\beta(s)$ curve starts to decrease with decreasing s before reaching a constant value that can be < 0.5 for K, G or F stars, thus placing sub-micron grains on bound orbits (Johnson et al., 2012). Another possibility is that we are witnessing a powerful collisional chain-reaction, called an "avalanche", of high-β particles passing through a dense ring of larger grains (Grigorieva et al., 2007).

1.1. Discs with "too large" minimum dust sizes

We will focus here on the opposite problem, i.e., the systems for which the observationally derived s_{min} has been found to be *larger* than s_{blow}. The existence of such systems was first unambiguously determined by Pawellek et al. (2014), who consid-

Send offprint requests to: P. Thebault
Correspondence to: philippe.thebault@obspm.fr

[1] For subsolar stars, radiation pressure is too weak to overcome gravity, but stellar wind could play a similar role for active M stars like AU Mic (Augereau & Beust, 2006; Schüppler et al., 2015)

ered a sample of 34 resolved discs [2] and found that, while discs around A-star have $s_{min} \sim s_{blow}$, the s_{min}/s_{blow} ratio increased towards low-mass stars and could reach $\sim$ 10 for solar-type stars. These results were later confirmed by Pawellek & Krivov (2015), who showed that the s_{smin}/s_{blow} trend is robust and does not depend on material compositions or grain porosity.

These results seem to be in contradiction with the aforementioned behaviour expected in discs where a size distribution in $dN \propto s^q ds$ holds down to the blow-out size s_{blow}, for which luminosities should be dominated by grains close to the blow-out size. Interestingly, numerical investigations of the collisional evolutions of debris discs have shown that, at least in the small-size domain, size distributions can in fact significantly depart from an idealized $dN \propto s^q ds$ power-law. The simulations of Thebault et al. (2003); Krivov et al. (2006); Thebault & Augereau (2007) have indeed shown that size-distributions can exhibit pronounced "wavy" patterns in the $\lesssim 100 s_{blow}$ domain, triggered by the absence of potential destructive projectiles below s_{blow}. However, this waviness cannot deprive the system from grains close to s_{blow}, and it even generally has just the opposite effect, inducing a density peak of grains in the $1.5 - 2 s_{blow}$ region (Thebault & Augereau , 2007).

A possible cause of small-grain depletion could be the well known Poynting-Robertson drag causing small particles to slowly spiral starwards. However, this effect is likely to only be noticeable for tenuous discs for which the collisional timescale of small grains becomes larger than t_{PR} (Wyatt, 2005). The first plausible mechanism for small-grain depletion that could also work for bright discs was proposed by Thebault & Wu (2008), who showed that, in discs with a low dynamical excitation (low orbital eccentricities e and inclinations i), there is an imbalance between the production and destruction rates of small grains. Indeed, while their production rate is controlled by the erosion of larger particles and is thus low because of these particles' low $<e>$, their *destruction* rate, which is controlled by impacts involving the small grains themselves, is much higher because these grains are placed on high-e orbits by radiation pressure regardless of the dynamical excitation in the rest of the system. As a result, depending on the value for $<e>$, there could be a strong depletion of grains up to sub-mm sizes. The main issue with this scenario is that it requires values of $<e>$ that could possibly be unrealistically low (see Sec.4).

1.2. Maximum surface energy and minimum fragment size

Another, potentially more generic scenario has been recently proposed by Krijt & Kama (2014). It is based on an energy-conservation criteria, related to the physics of collisions themselves, which had, remarkably enough, never been invoked before in the context of debris discs. The argument is that a destructive collision cannot produce a size distribution of fragments that reaches an infinitely small value, as this would require an infinite amount of energy. This is because creating new fragments means increasing the amount of exposed surface, and this requires energy. There is thus a minimum size s_{surf} in the fragment distribution, given by the requirement that the total surface energy of all fragments cannot exceed the kinetic energy of the impact. For the specific case of a fully destrictive impact between two equal-sized bodies and for a $q = -3.5$ size distribution, Krijt & Kama (2014) derived a relation linking s_{surf} to s_{lfr}, the size of the largest fragment, and the impactor's size s_0:

$$s_{surf} = \left(\frac{24\gamma s_0}{\eta \rho s_0 v_{rel}^2 + 24\gamma} \right)^2 s_{lfr}^{-1} \quad (1)$$

where v_{rel} is the impact velocity, γ is the surface energy per unit surface, and η if the fraction of the kinetic energy that is used for creating new surface. Interestingly, this formula gives the counter-intuitive result that, for a a given v_{rel} and a fixed s_{lfr}/s_0 ratio (i.e., for self-similar impacts), the size of the smallest fragment *increases* with decreasing s_0 sizes. For low-velocity impacts, low values of η and for material with high γ (like ice), s_{surf} can be significantly higher than s_{blow} for $s_0 \lesssim 1$ m (see Fig.1 of Krijt & Kama, 2014).

However, while deriving estimates of s_{surf} is analytically possible for one given collision, given global estimates for a whole debris disc is a much more problematic task, as the values of s_{surf} will strongly vary depending on the absolute and relative sizes of the impacting objects. In their pioneering study, Krijt & Kama (2014) did an attempt at deriving a disc-integrated s_{surf} by only considering impacts between equal-sized s_0 objects and by restricting themselves to "barely catastrophic" impacts where each impactor is split into 2 identical fragments. This simplifying choice relied on two main assumptions: 1) For a given target size, and if s_{lfr} *is fixed*, it is with a projectile of the same size that the smallest "smallest fragments" should be obtained, hence the choice of equal-sized impacts as the most constraining ones, and 2) in a collisional cascade, small grains should preferentially originate from collisions involving particles barely larger than themselves; so that even if collisions amongst large objets have very small s_{surf} values (because $s_{surf} \propto s_0^{-1}$ if s_{lfr}/s_0 is fixed) the amount of small dust they produce cannot compensate for the amount of small dust "not produced" (because of their larger s_{surf}) by collisions amongst small grains, hence the focus on the smallest "barely catastrophic" impacts . Under these simplifying hypothesis, the disc-integrated s_{surf}^{DD} is then the s_{surf} obtained for the smallest s_0 object that can be split in 2 by an impact at v_{rel}:

$$\frac{s_{surf}^{DD}}{s_{blow}} = 2.4 \left(\frac{r}{5\mathrm{AU}} \right) \left(\frac{L_*}{L_\odot} \right)^{-1} \left(\frac{f}{10^{-2}} \right)^{-2} \left(\frac{\eta}{10^{-2}} \right)^{-1} \left(\frac{\gamma}{0.1\mathrm{J.m}^{-2}} \right) \quad (2)$$

where $f = (1.25e^2 + i^2)^{0.5}$.

1.3. Need for a numerical approach

As rightfully underlined by Krijt & Kama (2014) themselves, Equ.2 should only be taken as an order of magnitude estimate, as it only takes into account a very limited range of collision types. But even this role as an order-of-magnitude indication should be taken with caution, because the simplifying assumptions justifying the predominant role of equal-sized barely-catastrophic impacts might not hold in a realistic disc. The first problem is that this predominant role has been inferred assuming that s_{lfr} is fixed, which is far from being the case in realistic conditions, for which s_{lfr} strongly depends on the impactors mass ratio and on v_{rel} (e.g. Leinhardt & Stewart, 2012). Another problem is that it was derived assuming that a $q = -3.5$ power-law holds for the whole size distribution, which several debris disc studies have shown to be erroneous, especially in the small grain size domain. Last but not least, it neglects the contribution of *cratering* impacts, which might have a dominant role in the global dust pro-

[2] There is an inherent degeneracy between grain size and disc radius that can only be broken for resolved systems (see discussion in Pawellek & Krivov, 2015)

duction and destruction balance (Thebault & Augereau , 2007; Kobayashi & Tanaka, 2010) [3].

Pawellek & Krivov (2015) improved on Equ.2 by taking into account the fact that velocities of impacts involving small grains might have higher values because radiation pressure places small grains on highly eccentric or even parabolic orbits. This significantly reduced the values of s^{DD}_{surf}/s_{blow} with respect to Equ.2. Interestingly, this did, however, not improve the fit to the observationally-derived s^{DD}_{surf}/s_{blow}, for which the original Krijt & Kama (2014) formula seems to provide a better match (see Fig.14 of Pawellek & Krivov, 2015). However, even the improved formula used by Pawellek & Krivov (2015) is still a disc-averaged analytical estimate relying on the same simplifying assumptions mentioned earlier.

We propose here to take these studies a step further by incorporating, for the first time, the surface-energy constraint *within* a numerical collisional evolution code, estimating s_{surf}(i,j) for all pairs of impacting bodies of sizes s_i and s_j and taking these values into account in the collision-outcome prescription of our code. We describe our numerical model and the set-ups for the different cases that we explore in Sec.2. Results are presented in Sec.3, where we first compare the s_{surf}(i,j) maps to equivalent (s_i,s_j) maps for the level of dust production in the disc. We then display the steady state particle size distributions obtained for all considered cases, and investigate the signature of the surface-energy constraint by comparing these PSDs to those obtained for control runs without the s_{surf} criteria. We then discuss in Sec.4 the importance of the surface-energy constraint, in particular with respect to the concurrent "low-stirring" dust-depletion mechanism identified by Thebault & Wu (2008).

2. Model

We use the statistical collisional model developed by Thebault et al. (2003) and later upgraded by Thebault & Augereau (2007). It has a "particle-in-a-box" structure, where particles are sorted into logarithmic size bins separated by a factor 2 in mass. It has also a 1D spatial resolution, being divided into radially concentric annuli. Collisions rates between all size bins are computed using an estimate of the average orbital eccentricity and inclinations in each size bin. Crucially, the code takes into account the increased eccentricities, and thus impact velocities of small grains whose orbits are affected by stellar radiation pressure, as well as the fact that these grains are able to cross several concentric annuli (see Appendix of Thebault & Augereau, 2007). Collision outcomes are then divided into two categories, cratering and fragmentation, depending on the ratio between the specific impact kinetic energy and the specific shattering energy $Q*$, which depends on object sizes and composition. In both regimes, the size of the largest fragment and the size distributions of the other debris are derived through the detailed energy scaling prescriptions presented in Thebault et al. (2003) and Thebault & Augereau (2007).

The main upgrade for the present runs is that we implement a prescription for s_{surf}. We derive s_{surf}(i, j) for all possible colliding pairs of sizes s_i and s_j and implement this parameter into our collision-outcome prescription: if, for a given collision between the bins "i" and "j", s_{surf}(i, j) > $s_{min-num}$ (where $s_{min-num}$ is the smallest size bin considered in the code), we cut the post-impact fragment distribution at s_{surf}(i, j) instead of $s_{min-num}$.

Table 1. Set-up for the numerical simulations. γ is the surface energy per surface unit of material and η is the fraction of the kinetic energy that is used for creating new surface.

$s_{min-num}$	s_{blow}
$s_{max-num}$	50m
Initial mass	$0.01 M_{\oplus}$
r_{min}	50 AU
r_{max}	100 AU
$L^*/L_{\odot}$	1 or 9
$<e>$	0.075 or 0.01
$Q*$ prescription	Benz & Asphaug (1999) (for basalt)
s_{surf}	Appendix of Krijt & Kama (2014)
γ	$0.74\,\mathrm{J.m^{-2}}$
η	0.01

We estimate the values of s_{surf}(i,j) for both fragmenting and cratering impacts, using the equations presented in the Appendix of Krijt & Kama (2014):

$$s_{surf} = \left[\frac{6\gamma \left(s_i^3 + s_j^3\right)^2}{\eta \rho v_{rel}^2 (s_i s_j)^3} \right]^2 s_{lfr}^{-1} \quad \text{for fragmentation} \qquad (3)$$

$$s_{surf} = \left(\frac{6\gamma\kappa}{\eta \rho v_{rel}^2} \right)^2 s_{lfr}^{-1} \quad \text{for cratering} \qquad (4)$$

where we assume that i is the target and j the projectile ($s_i \geq s_j$). For the cratering case, κ is the ratio m_{crat}/m_j, where m_{crat} is the total mass excavated from the target i. The crucial point is here that, instead of having to *assume* values for the largest fragment's size s_{lfr} and the ratio κ, we can retrieve both quantities in a self-consistent way from our collision-outcome prescription.

2.1. set-up

We do not consider the full range of possible $L^*/L_{\odot}$ explored by Pawellek & Krivov (2015), but restrict ourselves to the two illustrative cases of a sun-like $L^* = L_{\odot}$ star and a β-Pic-like A5V star with $L^* = 9L_{\odot}$. We consider a reference debris disc extending from $r_{min} = 50$ AU to $r_{max} = 100$ AU. The disc's total initial mass is $M_{disc} = 0.5 M_{\oplus}$, distributed between $s_{max-num} = 50$m and $s_{min-num} = s_{blow}$, which corresponds to $\sim 0.01 M_{\oplus}$ of < 1mm dust[4]. The value of s_{blow} is equal to 0.5μm for the sun-like case (with 80 size bins from s_{max} to s_{blow}) and 4μm for the A star one (71 size bins). As for the dynamical state of the disc, we consider one dynamically "hot" case with $< e >= 0.075$ and one dynamically "cold" case with $< e >= 0.01$. For each L^* and $< e >$ case, we run both a simulation taking into account the s_{surf} prescription and a reference case with no s_{surf}. We let the runs evolve for 10^7years, which is enough to reach a collisional steady-state in the dust size domain (< 1 cm).

As for the free parameters of the s_{surf} prescriptions (Equs.3 and 4), we adopt a conservative approach and chose, amongst the η and γ values considered by Krijt & Kama (2014), the ones that are in principle the most favourable to yielding large s_{surf} values. We thus take $\eta = 0.01$ (i.e., 1% of the kinetic energy is

[3] To their credit, Krijt & Kama (2014) briefly investigate the role of cratering impacts in their Appendix, but again assuming a fixed s_{lfr}/s_{target} ratio (see Fig.B.1. of that paper)

[4] The value for M_{disc} is not a crucial parameter, as it will only affect the timescale for the disc evolution without affecting the results (s_{surf}(i,j) and dust production maps, PSDs) obtained at steady-state

Table 2. Main results for all four collisional runs. s^{DD}_{surf}/s_{blow} is the simplified analytical value given by Equ.2. $\Delta M_{s\leq 2s_{blow}}$ and $M_{4s_{blow}\leq s\leq 20s_{blow}}$ are the relative amount of "small-" and "medium"-sized dust, respectively, as compared to a control simulation with no constraint on s_{surf}.

$L^*/L_\odot$	<e>	s_{blow}	s^{DD}_{surf}/s_{blow}	$\Delta M_{s\leq 2s_{blow}}$	$\Delta M_{4s_{blow}\leq s\leq 20s_{blow}}$
9	0.075	4μm	0.4	-0.038	+0.074
9	0.01	4μm	19.8	-0.049	+0.199
1	0.075	0.5μm	3.1	-0.277	+0.410
1	0.01	0.5μm	153	-0.127	+0.145

used for creating new surface) and $\gamma = 0.74$J.m^{-2}, which is the value for water ice [5].

All main parameters for the set-up are summarized in Tab.1.

3. Results

3.1. Dust progenitors and s_{surf} maps

Fig.1 presents, for each of the considered set-ups, the s_{surf}(i, j) value for every pair of impacting target and projectile of sizes s_i and s_j. We also show, as a useful comparison tool, the equivalent (s_i,s_j) maps of the amount of μm-sized dust produced as a function of target and projectile sizes (Fig.2).

3.1.1. A-star

For the dynamically "hot" (<e>= 0.075) A-star case, Equ.2 predicts a low s^{DD}_{surf}/s_{blow} of only $\sim$ 0.4, and our s_{surf}(i, j) map is in good agreement with this prediction, as almost all (i,j) impacts result in $s_{surf}/s_{blow} < 1$ (Fig.1a) . There is, admittedly, a very narrow range of impacts for which $s_{surf}/s_{blow} \geq 1$, but even there the ratio does not exceed 2. Moreover, this limited family of $s_{surf} > s_{blow}$ collisions corresponds to a region that has only a very limited contribution to the global dust production. The dust production is instead dominated by impacts involving $s \sim s_{blow} = 5\mu$m projectiles and larger $5s_{blow} \lesssim s \lesssim 20s_{blow}$ targets (see Fig.2a). This is because $s \sim s_{blow}$ grains are placed on high-*e* orbits par radiation pressure and impact all other grains at very high velocities. They are thus very efficient at fragmenting targets, and producing dusty debris, over a wide range of target sizes.

The situation is slightly different for the dynamically "cold" A-star case, for which the fraction of $s_{surf}>s_{blow}$ impacts is more extended and the maximum value for s_{surf}(i, j) reaches $\sim$ 5 (Fig.1b). This value is, however, well below the analytical prediction $s^{DD}_{surf} \sim 20s_{blow}$ of Equ.2. We note that these high-s_{surf}(i,j) impacts are located close the $s_i = s_j$ diagonal, which could appear to contradict Fig.B.1 of Krijt & Kama (2014) showing instead a *minimum* of the s_{surf} curve for equal-sized impactors. But this is because this analytically-derived curve is only valid for *fragmenting* impacts, whereas here, with <e>= 0.01, the high-collisional-energy requirement for fragmentation can only be met when projectiles have sizes comparable to the target. All other cases result in cratering, for which s_{surf} are, in general, much smaller. As was the case for the <e>= 0.075 run, the (i,j) region of high s_{surf} values does not match the region of highest dust production, which corresponds, here again, to fragmenting impacts by $s \sim s_{blow}$ projectiles on $5s_{blow} \lesssim s \lesssim 20s_{blow}$ targets (Fig.2b). Nevertheless, the contribution of the high- s_{surf} region is not fully negligible, so that we expect the maximum surface energy criteria to have at least some effect on the system's evolution.

3.1.2. Solar-type star

For a Sun-like star, orbital velocities are lower and collisions less energetic than for an A-star for equivalent orbital parameters. The s_{surf}/s_{blow} values are thus logically higher, as is clearly seen in Fig.1c and d. The $s_{surf}/s_{blow} > 1$ domain is much more extended than for an A star, with peak values reaching $\sim$ 25 for the <e>=0.075 case and even $\geq$ 100 for the dynamically cold case. As was already the case for the A-star runs, these peak s_{surf} values are located, in the (s_i,s_j) map, on a line corresponding to the transition from cratering to fragmenting impacts [6] . For the <e>=0.075 run, this transition always occurs for $s_j \leq 0.5s_i$, with a s_j/s_i ratio that is decreasing towards larger sizes following an approximate law in $s_2/s_1 \sim 0.4 - 0.1\log(s_2/10\mu\text{m})$[7]. For <e>=0.01, the peak s_{surf} line still corresponds to the fragmentation/cratering transition, but is now much closer to the $s_i = s_j$ diagonal, which reflects the fact that, for these lower impact velocities, it takes a larger projectile to fragment a given target.

Note also that, for both the <e>=0.075 and <e>=0.01 cases, there are no high s_{surf}/s_{blow} values for impactors $\lesssim 10\mu$m. This is due to the fact that such small grains have more energetic impacts (able to produce smaller fragments) because of their radiation-pressure-affected orbits. Incidentally, this $s \lesssim 10\mu$m region is the one where the μm-dust production is the highest (Fig.2c and d). This means that a large fraction of the dust-generating impacts are in fact able to produce fragments down to the blow-out size. The regions of high s_{surf}/s_{blow}>5 only contribute to approximately 20% of the $\leq 10\mu$m dust production for both the <e>=0.075 and <e>=0.01 cases.

3.2. size distribution

Figs.3 and 4 present the particle size-distribution (PSD), in terms of the differential distribution of geometric cross section $d\Sigma/ds$, at collisional steady-state[8], for all the 4 four explored set-ups, as well as for the control runs where the s_{surf} constraint is ignored. Visualizing the $d\Sigma/ds$ distribution allows to immediately identify which particle sizes dominate the system's optical depth, and thus its luminosity.

[5] We are aware that this value is not self-consistent with our values of s_{blow}, which are derived for astro-silicates. Nevertheless, this is in line with our choice of considering the maximum possible effect for the surface-energy constraint

[6] This relatively sharp transition at the cratering/fragmentation boundary is due to the discontinuity in Krijt & Kama (2014)'s s_{surf} prescriptions (Equs.3 and 4) at this boundary ($s_{lfr} = 2^{-1/3}s_1$). More refined and self-consistent s_{surf} prescriptions should probably be derived in the future, but we chose to stick to the laws given by Krijt & Kama (2014) for this exploratory work.

[7] This negative slope reflects the fact that, in the strength regime, the specific shattering energy $Q*$ decreases with increasing sizes (Benz & Asphaug, 1999)

[8] Or, more exactly, when steady-state is at least reached where it matters here, that is in the s<1cm domain. In the large-size domain, there is a difference of PSD slopes between the dynamically hot and cold discs that is due to the fact that the <e>=0.01 systems have not had time to reach collisional steady-state for these larger objects yet. Collisional steady-state does indeed work its way up the PSD with time, at a rate that strongly increases with decreasing dynamical stirring (e.g. Löhne et al., 2008).

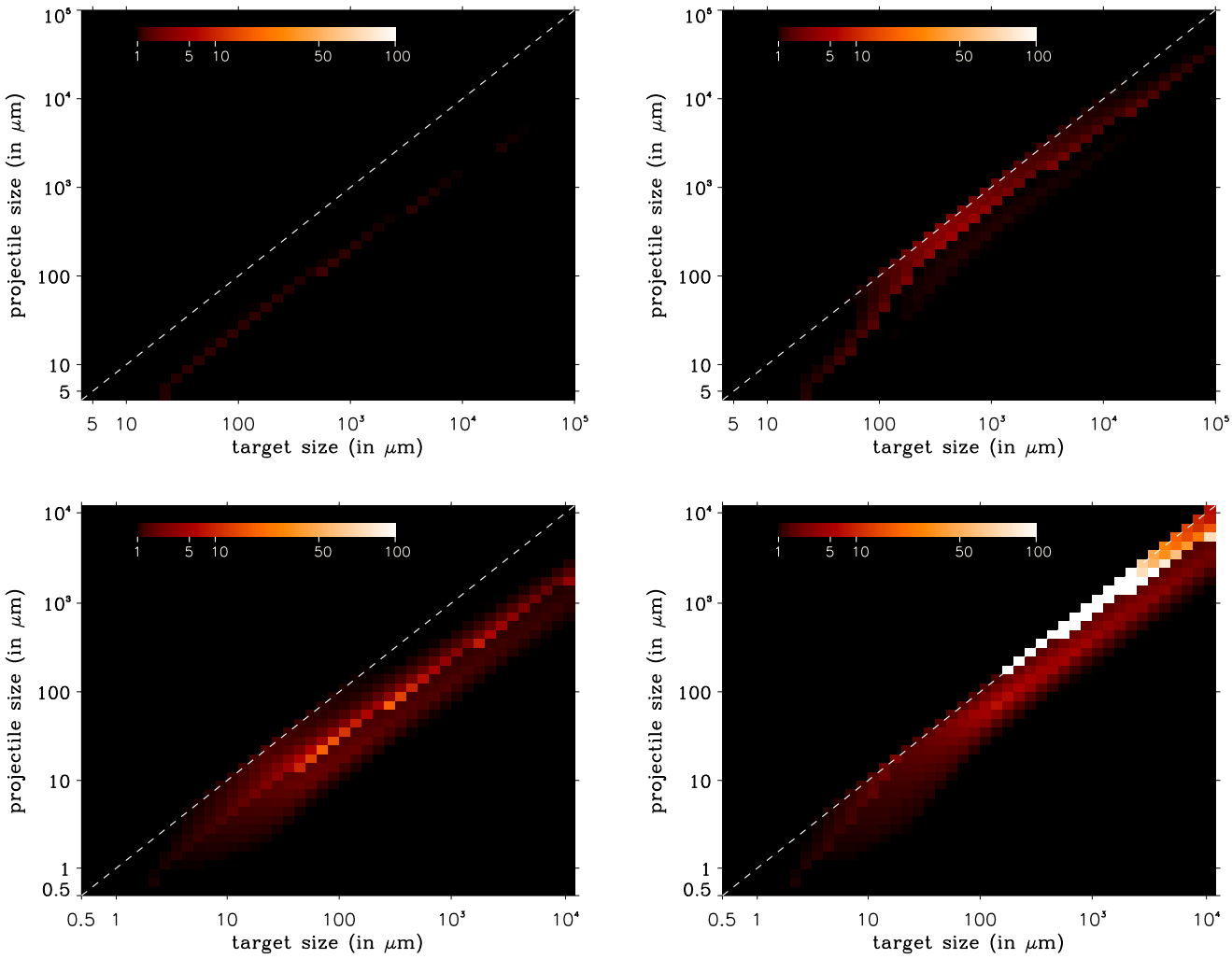

Fig. 1. Disc-integrated mean values of the s_{surf}/s_{blow} ratio for all possible target-projectile pairs of sizes s_i and s_j. *Upper left panel*: A-star primary and <*e*>=0.075. *Upper right*: A-star primary and <*e*>=0.01. *Bottom left*: solar-type primary and <*e*>=0.075. *Bottom right*: solar-type primary and <*e*>=0.01. The dashed white line delineates the $s_i = s_j$ diagonal of equal-sized impactors.

3.2.1. Generic features

Before assessing the additional effect of the s_{surf} constraint, let us first underline some characteristics of the obtained size distributions that are well known generic features of steady-state collisional discs that also affect the small-size domain of the PSDs.

A first "classical" result is that, for all cases, the size distribution displays a clear wavy structure in the $\lesssim 100\mu$m domain. This waviness is more pronounced than in Pawellek & Krivov (2015) because we consider a wider disc, so that small grains, placed on high-*e* orbits par radiation pressure, will be able to impact target particles at a higher impact angle and thus higher v_{rel}. This will reinforce their shattering power and thus the amplitude of the size distribution wave (see Thebault & Augereau , 2007, for a detailed discussion on "wave-enhancing" factors).

Another crucial result is the strong depletion of small particles for all <*e*>=0.01 cases. This is the signature of the mechanism identified by Thebault & Wu (2008), i.e., the strong imbalance between the small-dust production and destruction rates for dynamically cold systems (see Sect.1.1). As underlined by Pawellek & Krivov (2015), this effect is more pronounced for solar-type stars, for which we find a clear drop of the $d\Sigma/ds$ curve at $s \lesssim 50 s_{blow}$, than for A stars, where the PSD is roughly flat in the same $s \lesssim 50 s_{blow}$ domain. Nevertheless, for both cases the depletion of small grains is very strong, exceeding one order of magnitude as compared to a dynamically "hot" system.

3.2.2. Effect of the s_{surf} constraint

As expected from the s_{surf}(i, j) and dust-production maps (see Sec.3.1), the effect of the s_{surf} constraint is very weak for the A-star runs. For the <*e*>=0.075 case, the PSD is almost indistinguishable from the control run with s_{surf} switched off (Fig.3). Some differences between the with- and without-s_{surf} runs are visible for the <*e*>=0.01 case, but they remain relatively limited. Interestingly, they are not so much visible as a dearth of grains in the $s \leq 10-20\mu$m domain where the few $s_{surf} \geq s_{blow}$ values lie (see Fig.1b), but rather as an *excess* of larger particles in the ~30-50μm range. This is a direct consequence of the specific dynamics, and thus destructive efficiency, of grains close to s_{blow}. In the "s_{surf}-free" case, it is indeed this high destructive efficiency that is responsible for the strong depletion of $30-50\mu$m

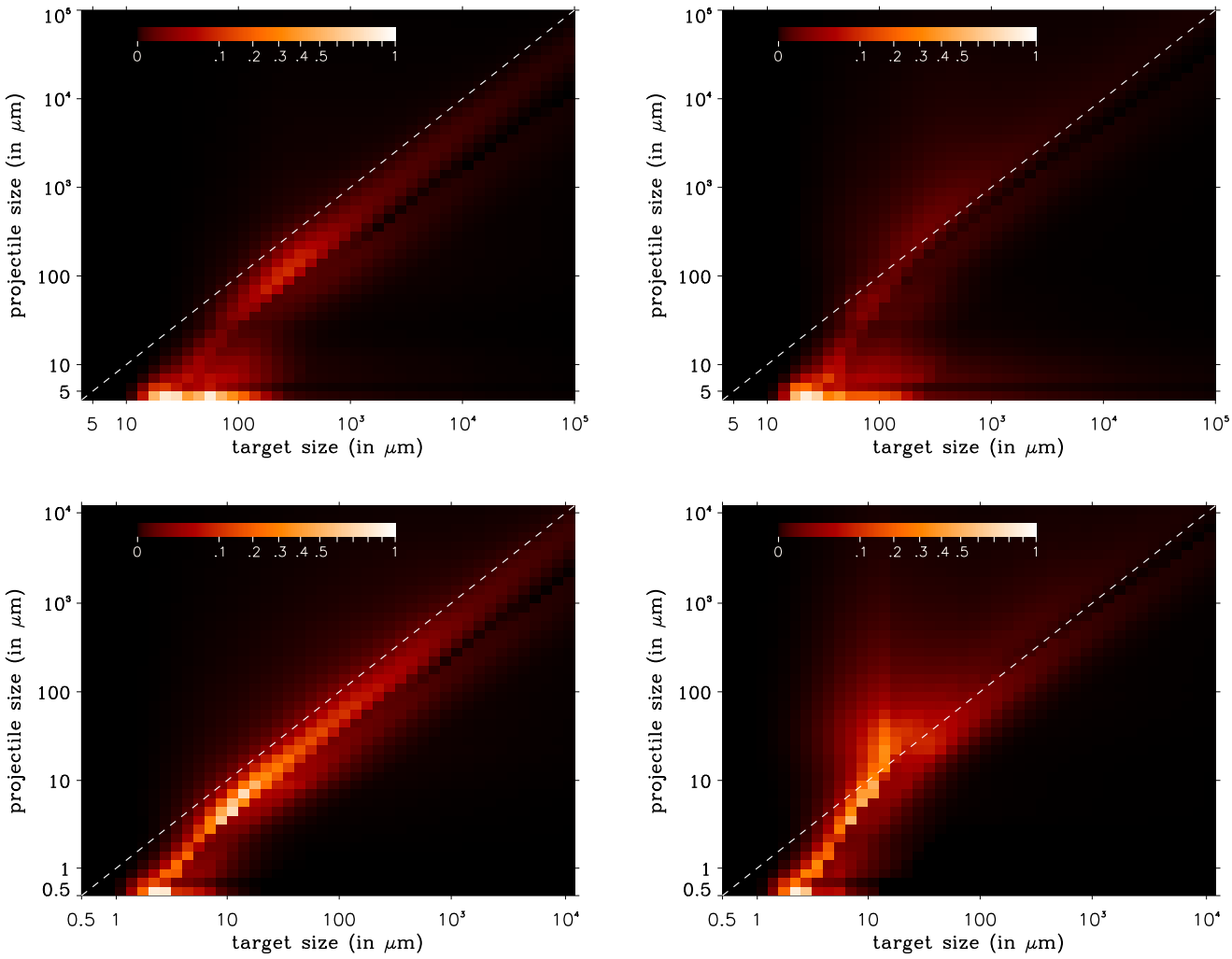

Fig. 2. Disc-integrated and normalized production rates of $s \leq 10\mu$m dust as a function of target and projectile sizes. These maps are estimated, at collisional steady-state, for the "control runs" where the s_{surf} criteria is turned off. This allows easy comparison with Fig.1 by directly showing which high s_{surf}(i,j) regions will have a significant damping effect on the small-dust production rate. *Upper left panel*: A-star primary and <*e*>=0.075. *Upper right*: A-star primary and <*e*>=0.01. *Bottom left*: solar-type primary and <*e*>=0.075. *Bottom right*: solar-type primary and <*e*>=0.01.

particles in the PSD (the first dip in the "wave")[9]. So removing a small number of small destructive impactors will necessarily increase the number of $30-50\mu$m grains. And given that we start from a strongly depleted population of $30-50\mu$m particles in the s_{surf}-free case, their *relative* increase in the s_{surf} runs will be higher than the relative decrease of $s \leq 10-20\mu$m grains. And this is exactly what we observe (see Tab.2): a $\sim$ 5% depletion of $s \sim s_{blow}$ grains that causes a $\sim$ 20% excess of $s \sim 30\mu$m particles, which is the size of the biggest objects that can be destroyed by projectiles close to s_{blow}. Note, however, that, for this <*e*>=0.01 case, the s_{surf}-induced depletions and excesses remain marginal when compared to the much more significant global depletion of $s \lesssim 50 s_{blow}$ grains caused by the low dynamical excitation of the system (see Discussion).

The imprint of the s_{surf} limit is, logically, much more visible around a Sun-like star (Fig.4). Interestingly, this is especially true of the dynamically hot disc, for which the depletion of $s \leq 2 s_{blow}$ grains is close to 30%, and the related excess of $4 s_{blow} \leq s \leq 20 s_{blow}$ particles exceeds 40% (Tab.2). For the <*e*>=0.01 run, these excesses and depletions are only $\sim$ 12% and $\sim$ 14%, respectively. This is a rather counter-intuitive result, as Equ.2 predicts a s_{surf}^{DD}/s_{blow} ratio 50 times higher for <*e*>=0.01 than for <*e*>=0.075, and even the more accurate Figs.1c and d show peak s_{surf}(i,j) values that are still 6-7 times higher for the dynamically cold case. However, as discussed in Sec.3.1.2, the crucial point is that these (s_i,s_j) regions of high s_{surf} values do *not* match those of high dust-production. Most of the dust is indeed created by collisions on $s \leq 10\mu$m ($\lesssim 20 s_{blow}$) targets (Fig.2), for which s_{surf} rarely exceeds s_{blow} (Fig.1). Another reason for which the s_{surf} constraint only leaves a weak signature on the <*e*>=0.01 system is that, in the $s \leq 100\mu$m range, the PSD is already massively depleted because of the dust-production imbalance inherent to dynamically "cold" discs. This effect is even stronger than for the A-star case, with a depletion that reaches almost 2 orders of magnitude for $s \sim s_{blow}$ grains (Fig.4).

[9] Note that the presence of a wave does not depend on the high-*e* orbits of small grains, but these high-*e* orbits, and thus high impact velocities, strongly increase the wave's amplitude

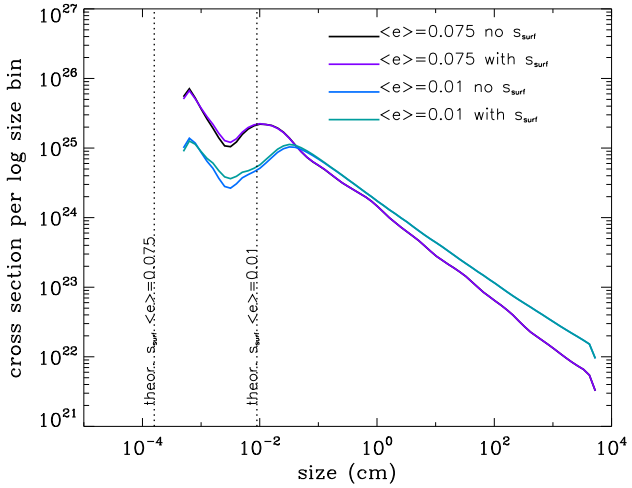

Fig. 3. A-star case. Geometrical cross section as a function of particle size, at $t = 10^7$ years, integrated over the whole 50-100 AU disc, for both the dynamically "hot" (<*e*>=0.075) and "cold" (<*e*>=0.01) cases. For each case, a reference run with the s_{surf} constraint switched-off is also presented. The two vertical dotted lines represent the analytical values given by Equ.2.

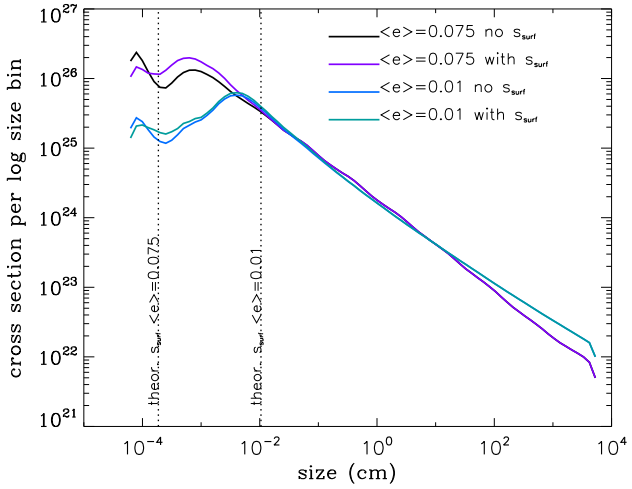

Fig. 4. Same as Fig.3, but for a solar-type star.

4. Discussion and Conclusion

Figs.3 and 4 seems to indicate that the two dynamically "hot" cases bear some similarities with the prediction of Equ.2 regarding the imprint of the s_{surf} constraint on the PSD. For the A-star case this similarity is of course simply that the surface energy constraint has no effect on the PSD, but for the <*e*>=0.01 case, we do indeed find a depletion of grains in the $s \leq 2s_{blow}$ domain, which is roughly consistent with the $s^{DD}_{surf}/s_{blow} \sim 3$ value given by Equ.2. However, this quantitative agreement is probably largely a coincidence, firstly because the depletion of $s \leq s_{surf}$ grains does not come from the "smallest-barely-catastrophic-equal-size-impactors" collisions considered in deriving Equ.2 (see Figs1c and 2c), and secondly because this depletion stops at $s \sim 2s_{blow}$ largely because of the "natural" waviness of the PSD combined to the *excess* of $\geq 3s_{blow}$ particles. We also note that this depletion is limited to $\sim$ 30% and does not create a sharp cut-off in the size distribution. This limited amplitude, combined to the aforementioned excess of particles in the $\sim 3s_{blow}$ to ~20-30s_{blow} range, renders the PSD plateau-like at sizes smaller than $\sim 10s_{blow}$. It is thus difficult to define a proper s_{min} for the size distribution, but, at least from a qualitative point of view, we confirm that, for this case, the maximum energy criteria does have a visible effect on the lower-end of the PSD.

The situation is radically different for the dynamically cold cases, for which the simulated size distributions are much less affected by the s_{surf} constraint than what could be expected from simple analytical estimates, which predict s^{DD}_{surf}/s_{blow} values in excess of 20, or even 150 (see Tab.2). Even though we do find some (s_i,s_j) target-projectile configurations that result in large s_{surf} comparable to these values (Fig.1), the decisive point is that these collisions only have a marginal contribution to the disc's total small-dust production. As a result, the differences with the reference s_{surf}-free cases' PSDs remain very limited: neither for the A-star nor for the Sun-like cases do we obtain a depletion that exceeds $\sim$ 10% in the small grain domain close to s_{blow}. Crucially, the s_{surf} constraint is never strong enough to change the size of grains that dominate the system's geometrical cross section, and thus its luminosity.

More importantly, we confirm that the most efficient way of depleting a collisional debris disc from its small grains is, by far, to reduce its dynamical excitation. The production/destruction imbalance mechanism identified by Thebault & Wu (2008) for low-stirring discs has an effect that exceeds, by more than one order of magnitude, that of the s_{surf} limit. This is both true for the amplitude of the small-grain depletion and for the size-range that is affected. For low <*e*> values, the size s_{cold} below which the PSD is depleted is, to a first order, given by the relation

$$\frac{\beta(s)}{1-\beta(s)} = < e > \qquad (5)$$

which translates into

$$s_{cold} = \frac{1 + < e >}{2 < e >} \; s_{blow} \qquad (6)$$

leading to $s_{cold} \sim 50s_{blow}$ for our <*e*>=0.01 case, a value that roughly agrees with the one obtained in the simulations (Figs.3 and 4). It should be noted that this dominance of the low-stirring imbalance effect over the surface energy constraint is probably even stronger than what we witness in Figs.3 and 4, since we have taken, for our s_{surf} prescription, the parameters that were the most likely to lead to high s_{surf} values (see Sec.2.1). On a related note, choosing disc configurations enhancing the amplitude of the surface-energy constraint, by for instance decreasing <*e*> or increasing [r_{min}, r_{max}], would not change this dominance either, because these configurations would *also* enhance the dust-production-imbalance effect by further decreasing the level of stirring in the disc.

We stress that we did not here attempt to fit observed s_{min}/s_{blow} trends with an exhaustive parameter exploration (<*e*>, M_{disc}, [r_{min}, r_{max}], etc.) in the spirit of the Pawellek & Krivov (2015) study. Our goal was here to quantify, in a self-consistent way, the relative effects of the two potential dust-depletion mechanisms that are the surface energy constraint and the low-stirring dust-production imbalance. For the sake of clarity, and to clearly identify the mechanisms at play, we restricted our study to a reference wide disc and to the two illustrative reference cases of a sun-like and an A-type star. Test runs with a narrower, ring-like disc, have, however, been performed. They

gave relatively similar results as to the relative imprint of the s_{surf} and low-stirring effects on the PSD, although with a less pronounced waviness in the PSD's shape, which was to be expected, as small grains close to s_{blow} will impact larger targets within a narrow ring at a lower velocity than they would have in an extended disc.

Despite this limited parameter exploration, we note, however, that our conclusions seem to agree with the numerical investigations of Pawellek & Krivov (2015), who were able to find a reasonable fit to the s_{min}/s_{blow} trend observed on their 34-stars sample with the low-stirring-induced mechanism *alone*. The main assumption for this fit to work is that, while the dynamical stirring of A stars should be of the order of $e \sim 0.1$, it should decrease towards lower mass stars and be as low as ~ 0.01 for solar-type objects. Such values might appear unrealistically low if we assume the classical view that debris discs are stirred by large Lunar-to-Mars-sized large planetesimals (e.g., Thebault , 2009). However, the level and the cause of stirring is still an open issue in present debris discs studies (see discussion in Pawellek & Krivov, 2015). Moreover, we know of at least two discs, around the G0V-star HD207129 (Löhne et al., 2012), and the K2V-star HIP17429 (Schüppler et al., 2014), for which collisional modelling predicts <*e*> barely larger than 0.01.

5. Summary

Based on analytical considerations, the pioneering study of Krijt & Kama (2014) found that the surface energy constraint, which limits the size of the smallest fragment produced after destructive collisions, could potentially affect the evolution of debris discs by limiting the smallest sizes of observable grains to a value s_{surf} larger than the blow-out size s_{blow}.

Here we numerically quantify the importance of this mechanism by incorporating, for the first time, the surface energy constraint into a statistical code following the collisional evolution of a debris disc. Instead of relying on an analytical system-averaged value, we compute s_{surf}(i,j) for all impacting target-projectile pairs of sizes s_i and s_j in the disc. We consider two stellar types, sun-like and AV5, and two levels of stirring for the disc, <*e*>=0.075 and <*e*>=0.01. Our main results and conclusions are the following:

- We confirm that, for all considered set-ups, there is a fraction of the (s_i,s_j) space for which $s_{surf} \geq s_{blow}$, especially for low <*e*> and/or low-mass stars.
- However, the (s_i,s_j) regions of high s_{surf} do *not* coincide with the regions of high dust production. Indeed, most of the μm-sized dust is produced by impacts involving $\sim$3-20s_{blow} targets and small $\lesssim$2-3s_{blow} projectiles, for which s_{surf} is in general smaller than the blow-out size. This is mainly due to the fact that impacts involving small grains are very energetic, because these particles are placed on high-*e* orbits by radiation pressure
- Because of this discrepancy between high-s_{surf} and dust-producing collisions, the global effect of the surface energy constraint is generally relatively limited. The only set-up for which it has a visible signature on the Particle Size Distribution (PSD) is for a dynamically "hot" disc around a solar-type star. But even there, the depletion of small dust does not exceed 30%.
- For the low <*e*>=0.01 cases, which should in principle be the most favourable to strong surface-energy constraints, the depletion of small grains never exceeds 12% and is never able to change the sizes of particles that dominate the system's geometrical cross section.
- At such low-stirring levels, the system's PSD in the small size domain is instead totally dominated by another mechanism: the imbalance between small-dust production and destruction rates identified by Thebault & Wu (2008) for low-*e* discs. This imbalance creates a depletion of small grains that is at least one order of magnitude more pronounced than the one caused by the surface-energy constraint, and it affects grains over a much wider size range.

Even if its effect is not as decisive as what could be analytically expected, we do, however, recommend to implement the surface-energy constraint in collisional-evolution codes, as it might leave visible signatures in the low-*s* end of PSDs for some star-disc configurations.

References

Ardila, D. R.; Golimowski, D. A.; Krist, J. E.; Clampin, M.; Williams, J. P.; Blakeslee, J. P.; Ford, H. C.; Hartig, G. F.; Illingworth, G. D., 2004, ApJ, 617, 147

Augereau, J. C., Lagrange, A. M., Mouillet, D., Papaloizou, J. C. B., & Grorod, P. A. 1999, A&A, 348,557

Augereau, J.-C., Beust, H., 2006, A&A, 455, 987

Benz, W., & Asphaug, E. 1999, Icarus, 142, 5

Dohnanyi J.S., 1969, JGR 74, 2531

Draine, B. T. 2003, ARA&A, 41, 241

Fitzgerald, Michael P.; Kalas, Paul G.; Graham, James R., 2007, ApJ, 670, 557

Fujiwara, A., Kamimoto, G., & Tsukamoto, A. 1977, Icarus, 31, 277

Grigorieva, A., Artymowicz, P., Thebault, P., 2007, A&A, 461, 537

Johnson, B. C., Lisse, C. M., Chen, C. H., et al. 2012, ApJ, 761, 45

Kobayashi, H., Tanaka, H., 2010, Icarus, 206, 723

Krijt, S., Kama, M., 2014, A&A, 566, 2

Krivov, A. V., Löhne, T., Sremcević, M., 2006, A&A, 455, 509

Krivov, A. V. 2007, in 3dust in Planetary Systems", Krueger., H., & Graps, A. Editors, p123.

Krivov, A. V. 2010, Research in Astronomy and Astrophysics, 10, 383

Leinhardt, Z. M., & Stewart, S. T. 2012, ApJ, 745, 79

Lisse, C. M., Chen, C. H., Wyatt, M. C., et al. 2009, ApJ, 701, 2019

Löhne, T., Krivov, A. V., & Rodmann, J. 2008, ApJ, 673, 1123

Löhne, T., Augereau, J.-C.; Ertel, S.; Marshall, J. P.; Eiroa, C.; Mora, A.; Absil, O.; Stapelfeldt, K.; Thebault, P.; Bayo, A, J., and 11 co-authors, 2012, A&A, 537, 110

Pawellek, Nicole; Krivov, Alexander, Marshall, Jonathan P.; Montesinos, Benjamin; Abrahám, Pter; Moór, Attila; Bryden, Geoffrey; Eiroa, Carlos, 2014, ApJ, 792, 65

Pawellek, Nicole; Krivov, Alexander, 2015, MNRAS, in press

Schüppler, Ch., Löhne, T., Krivov, A. V.; Ertel, S.; Marshall, J. P.; Eiroa, C., 2014, A&A, 567, 127

Schüppler, Ch., Löhne, T., Krivov, A. V.; Ertel, S.; Marshall, J. P.; Wolf, S.; Wyatt, M. C.; Augereau, J.-C.; Metchev, S. A., 2015, A&A, 581, 97

Thebault, P., Augereau, J. C., Beust, H., 2003, A&A, 408, 775

Thebault, P., 2009, A&A, 505, 1269

Thebault, P., Augereau, J. C., 2007, A&A, 472, 169

Thebault, P., Wu, Y., 2008, A&A, 481, 713

Wyatt, M. C. 2005, A&A, 433, 1007

Wyatt, M. C. 2008, ARA&A, 46, 339